THE ORBITAL MOTION IN LEO REGION: CBERS SATELLITES AND SPACE DEBRIS

Jarbas Cordeiro Sampaio [1a], **Rodolpho Vilhena de Moraes** [1b] **and Sandro da Silva Fernandes** [2c]

[1] *UNIFESP- Univ Federal de Sao Paulo, CEP. 12231-280 Sao Jose dos Campos, Brazil,*
[a] *jarbascordeiro@gmail.com* , [b] rodolpho.vilhena@gmail.com
[2] *ITA- Inst Tecnologico de Aeronautica, CEP. 12228-900 Sao Jose dos Campos, Brazil,*
[c] *sandro@ita.br*

Abstract: Synchronous satellites in circular or elliptical orbits have been studied in literature, due to the study of resonant orbits characterizing the dynamics of these satellites. In general, some resonant angles are considered in the numerical integration, with the purpose to describe the resonance defined by the commensurability between the mean motion of the object and the Earth's rotation angular velocity. However, the tesseral harmonics J_{lm} produce multiple resonances in the exact resonance and in the neighborhood of the exact resonance, and, some disturbances in the orbital motions of objects are not described. In this work, the CBERS satellites are studied observing resonance effects which compose your orbits. The time behavior of the orbital elements, resonant period and resonant angles are considered and possible regular and irregular motions are analyzed. The TLE (Two-Line Elements) of the NORAD (North American Defense) are studied observing the real orbital motions of the CBERS satellites. The Kozai's resonance is verified in the orbital motions of the CBERS-1 and CBERS-2 satellites.

Keywords: CBERS Satellites, Space Debris, Orbital Motion, Resonance.

1. Introduction

The objects orbiting the Earth are classified in Low Earth Orbit (LEO), Medium Earth Orbit (MEO) and Geostationary Orbit (GEO). Most of the objects are found in the LEO region. Considering approximately 10000 cataloged objects around the Earth, one can verify the distribution of objects as: 7 % of operational spacecraft, 22 % of old spacecraft, 41 % of miscellaneous fragments, 17 % of rocket bodies and about 13 % of mission-related objects. The uncatalogued objects larger than 1 cm are estimated in some value between 50000 and 600000 [1, 2].

Currently, the orbital motions of the cataloged objects can be analyzed using the 2-line element set of the NORAD (North American Defense) [3]. The TLE are composed by seven parameters and epoch. These data can be compared, for example, with the model of the orbit propagator situated in the artificial satellite. A similar study is done for the Brazilian satellite CBERS-1 in cooperation with China. In this case, orbital perturbations due to geopotential, atmospheric drag, solar radiation pressure, gravitational effects of the Sun and the Moon are considered in the numerical integration of the orbit and the results are compared with the TLE data [4].

In the last years, the LEO region have been studied about the space debris mitigation due to the increasing number of this kind of object through the years. These aspects englobe the observation, spacecraft protection and collision avoidance [5-9]

The present distribution of objects by the value of the mean motion n indicates the commensurability between the frequencies of the mean motion of the object and the Earth's rotation motion. It is verified that most of objects are in the region $13 \leq n(rev/day) \leq 15$.

The space between the Earth and the Moon has several artificial satellites and distinct objects in some resonance. Synchronous satellites in circular or elliptical orbits have been extensively studied in literature, due to the study of resonant orbits characterizing the dynamics of these satellites (see [10-21] and references here in)

In this work, resonant orbital motions of the CBERS satellites are studied using the TLE files of the NORAD. Figures show the time behavior of the semi-major axis, eccentricity, resonant angles and resonant periods. Figure 1 shows a design of the CBERS-2B satellite [22].

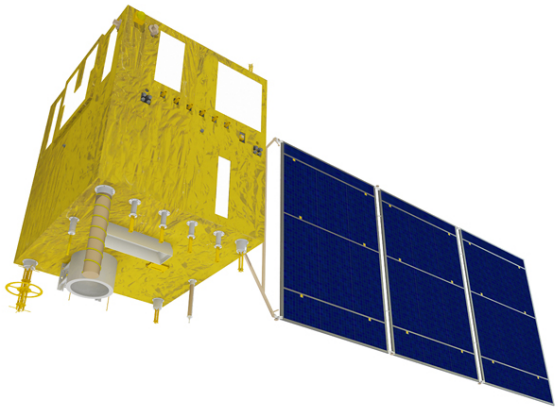

Figure 1: CBERS-2B Satellite.

2. Resonant orbital motions

In this section, the TLE data are used to verify objects in resonant orbital motions, specifically space debris and CBERS satellites around the 14:1 resonance [3].

To study the resonant objects using the TLE data, a criterium is established in the resonant period $Pres$, by the condition $Pres > 100$ days. Note that, the resonant period is related with a resonant angle which can influence the orbital motion of a particular object, a CBERS satellite or space debris for example. The value of $Pres$ helps to understand the influence of each resonant angle and a minimum value is established for the resonant period. $Pres$ is obtained by the relation,

$$Pres = \frac{2\pi}{\dot{\phi}_{lmpq}}. \tag{1}$$

and $\dot{\phi}_{lmpq}$ is calculated from [10].

$$\phi_{lmpq}(M, \omega, \Omega, \Theta) = (l - 2p + q)M + (l - 2p)\omega + m(\Omega - \Theta - \lambda_{lm}) \, . \tag{2}$$

with a, e, I, Ω, ω, M are the classical keplerian elements: a is the semi-major axis, e is the eccentricity, I is the inclination of the orbit plane with the equator, Ω is the longitude of the

ascending node, ω is the argument of pericentre and M is the mean anomaly, respectively; Θ is the Greenwich sidereal time and λ_{lm} is the corresponding reference longitude along the equator. So, $\dot{\phi}_{lmpq}$ is defined as

$$\dot{\phi}_{lmpq} = (l - 2p + q)\dot{M} + (l - 2p)\dot{\omega} + m(\dot{\Omega} - \dot{\Theta}) \ . \tag{3}$$

Substituting $k = l - 2p$ in (3),

$$\dot{\phi}_{kmq} = (k + q)\dot{M} + k\dot{\omega} + m(\dot{\Omega} - \dot{\Theta}) \ . \tag{4}$$

The terms $\dot{\omega}$, $\dot{\Omega}$ and $\dot{M}$ can be written as [6, 23].

$$\dot{\omega} = -\frac{3}{4} J_2 n_o \Big(\frac{a_e}{a_o}\Big)^2 \frac{(1 - 5cos^2(I))}{(1 - e^2)^2}.$$

$$\dot{\Omega} = -\frac{3}{2} J_2 n_o \Big(\frac{a_e}{a_o}\Big)^2 \frac{(cos(I))}{(1 - e^2)^2}.$$

$$\dot{M} = n_o - \frac{3}{4} J_2 n_o \Big(\frac{a_e}{a_o}\Big)^2 \frac{(1 - 3cos^2(I))}{(1 - e^2)^{3/2}}. \tag{5}$$

a_e is the Earth mean equatorial radius, a_e=6378.140 *km*, J_2 is the second zonal harmonic, $J_2 = 1,0826 \times 10^{-3}$.

The term $\dot{\Theta}$ in rad/day is

$$\dot{\Theta} \approx 1.00273790926 \times 2\pi. \tag{6}$$

In order to use orbital elements compatible with the way in which Two-Line Elements were generated, some corrections are done in the mean motion of the TLE data. Considering as n_1 the mean motion of the 2-line, the semi-major axis a_1 is calculated [6].

$$a_1 = \left(\frac{\sqrt{\mu}}{n_1}\right)^{2/3} \tag{7}$$

where μ is the Earth gravitational parameter, μ=3.986009 x 10^{14} m^3/s^2. Using a_1, the parameter δ_1 is calculated by the Eq. (8) [6].

$$\delta_1 = \frac{3}{4} J_2 \frac{a_e^2}{a_1^2} \frac{(3cos^2(I) - 1)}{(1 - e^2)^{3/2}}, \tag{8}$$

Now, the new semi-major axis a_o used in the calculations of the resonant period is defined using δ_1 from the Eq. (8) [6].

$$a_o = a_1 \left[1 - \frac{1}{3}\delta_1 - \delta_1^2 - \frac{134}{81}\delta_1^3 \right]. \tag{9}$$

and the new mean motion n_o used in the calculations is found considering the semi-major axis corrected a_o

$$n_o = \sqrt{\frac{\mu}{a_o^3}}. \tag{10}$$

The simulation identified CBERS satellites and space debris with resonant period greater than 100 days. Several values of the coefficients, k, q and m are considered in the Eq. (2) producing different resonant angles to be analyzed by the Eq. (1). See Tab. 1 showing details about the resonant angles used in the simulation.

Table 1: Coefficients k, m and q used in the simulation to verify resonant angles.

coefficient k	coefficient q	coefficient m
$-50 \leq k \leq 50$	$-5 \leq q \leq 5$	$1 \leq m \leq 50$

Fig. 2 shows the semi-major axis versus eccentricity of the objects in LEO region and Table 2 shows CBERS objects, including artificial satellites and space debris.

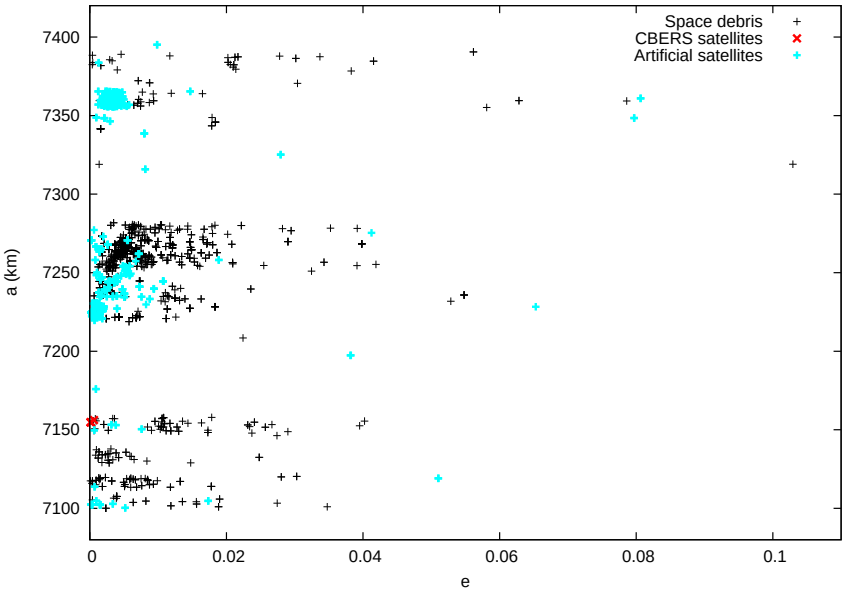

Figure 2: Semi-major axis versus eccentricity, of the objects in LEO region satisfying the criterion of the resonant period $Pres > 100 days$.

Table 2: CBERS Satellites and space debris

Object	Universal Code	Artificial Satellite (AS) or Space Debris (SD)
CBERS 1	25940	AS
CBERS 2	28057	AS
CBERS 2B	32062	AS
CBERS 1	30783	SD
CBERS 1	30789	SD
CBERS 1	30791	SD
CBERS 1	30792	SD
CBERS 1	31581	SD
CBERS 1	31582	SD
CBERS 1	31583	SD
CBERS 1	31586	SD
CBERS 1	31587	SD
CBERS 1	31588	SD
CBERS 1	31589	SD
CBERS 1	31590	SD
CBERS 1	31591	SD
CBERS 1	31592	SD
CBERS 1	31593	SD
CBERS 1	31594	SD
CBERS 1	31867	SD
CBERS 1	31869	SD
CBERS 1	31870	SD
CBERS 1	31871	SD
CBERS 1	31872	SD
CBERS 1	31873	SD
CBERS 1	31876	SD
CBERS 1	32064	SD
CBERS 1	32065	SD
CBERS 1	32067	SD
CBERS 1	32071	SD
CBERS 1	32072	SD
CBERS 1	32073	SD
CBERS 1	32074	SD
CBERS 1	32075	SD
CBERS 1	32076	SD
CBERS 1	32079	SD

These studies allow to investigate the real influence of the resonance effect in the orbital dynamics of the CBERS satellites and space debris. The number of resonant objects in comparison with the total number of objects in the TLE data shows the great influence of the commensurability between the mean motion of the object and the Earth's rotation angular velocity in its orbits.

In the next section, the orbital motions of CBERS-1 and CBERS-2 satellites are studied.

3. Orbital Motions of CBERS-1 and CBERS-2 satellites

In this section, the real data of CBERS-1 and CBERS-2 are used to study the possible regular or irregular orbital motions.

Figures 3 to 10 show the time behavior of the semi-major axis, eccentricity, resonant period and resonant angles of CBERS-1 and CBERS-2 satellites.

Observing the time behavior of the orbital elements of the objects CBERS-1 and CBERS-2 in Figs. 3 to 8, one can verify possible regular and irregular motions in the trajectories of these objects. The time behavior of the semi-major axis and eccentricity of the CBERS-2 show irregularities. Note that in 500 and 600 days, Fig. 7, a fast increase in the semi-major axis occurs and these variations is about 300 meters and it may be related with some disturbance added to the motion.

One can verify that the orbital dynamics of objects CBERS-1 and CBERS-2 are influenced by some resonant angles, which influence their orbits simultaneously.

If the commensurability between the orbital motions of the object and the Earth is defined by the parameter α and by the condition $\alpha = (k+q)/m$, one can say that the exact 14:1 resonance is defined by the condition $\alpha = 1/14$. This way, analyzing the Figures 6 and 10, it is verified that the motions of objects CBERS-1 and CBERS-2 are influenced by resonant angles in the neighborhood of the exact resonance.

Analyzing the time behavior of the resonant period in Figs. 5 and 9 it is verified that the resonant angles remain confined for a few days. The term confined means that the orbital motion is inside a region delimited for resonant angles with biggest resonant periods. Figures 6 and 10, corresponding to the objects CBERS-1 and CBERS-2 show a tendency to not remain in resonance, because the resonant period decreases from values greater than 10000 days to values smaller than 300 days.

To continue the analysis about the irregular orbital motions, the time behavior of the $\dot{\phi}_{kmq}$ is studied verifying if different resonant angles describe the orbital dynamics of these objects at the same moment.

Analyzing the time behavior of the resonant angles in Figs. 6 and 10, one can verify that all resonant angles have the same α, $\alpha = 3/43$ in different combinations for $(k+q)$. Objects CBERS-1 and CBERS-2 have their orbital motions influenced by resonant angles in the neighborhood of the exact 14:1 resonance and they need a full system with different resonant angles which compose their motions.

These discussions show the complexity in the orbital motions of these objects caused by the resonance effects. Furthermore, the increasing number of space debris and collisions between them can cause problems for artificial satellites missions.

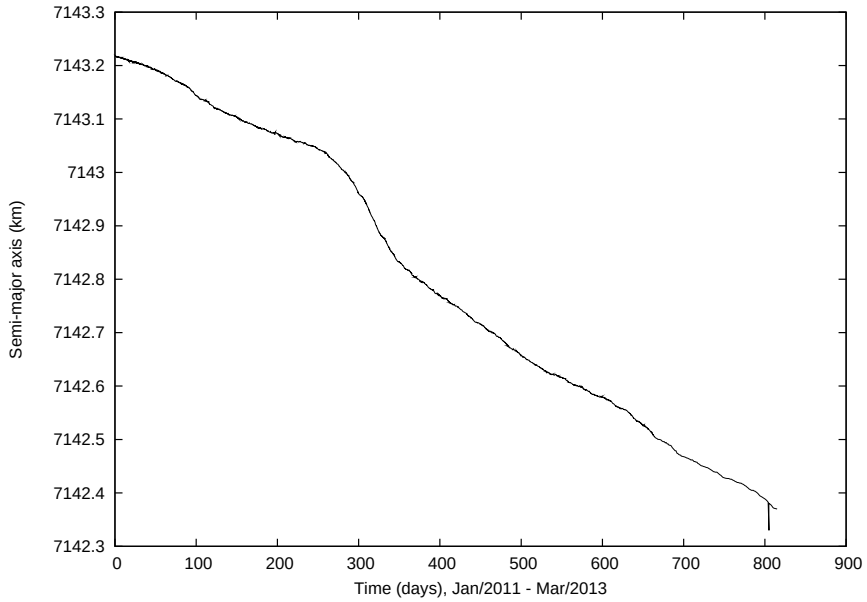

Figure 3: Time behavior of the semi-major axis: Orbital motion of the artificial satellite CBERS-1 corresponding to January/2011 to March/2013.

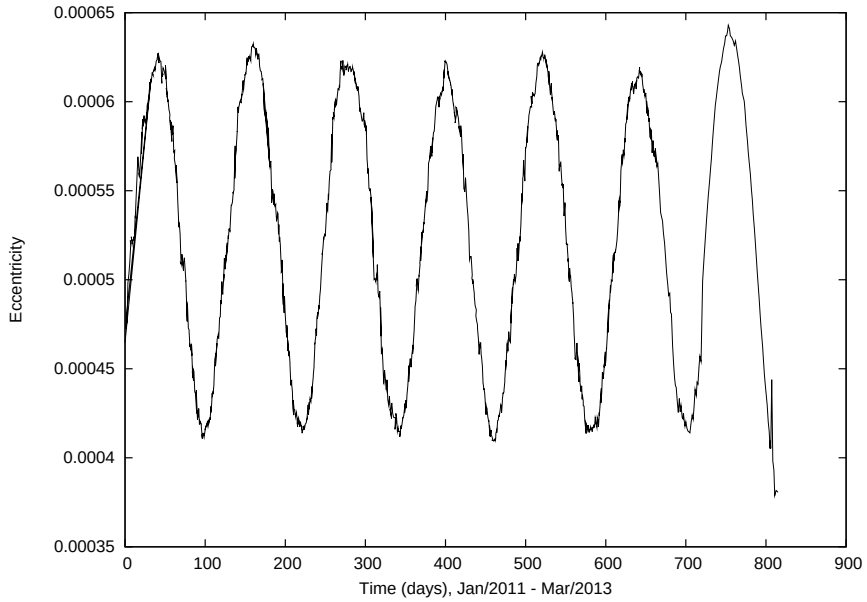

Figure 4: Time behavior of the eccentricity: Orbital motion of the artificial satellite CBERS-1 corresponding to January/2011 to March/2013.

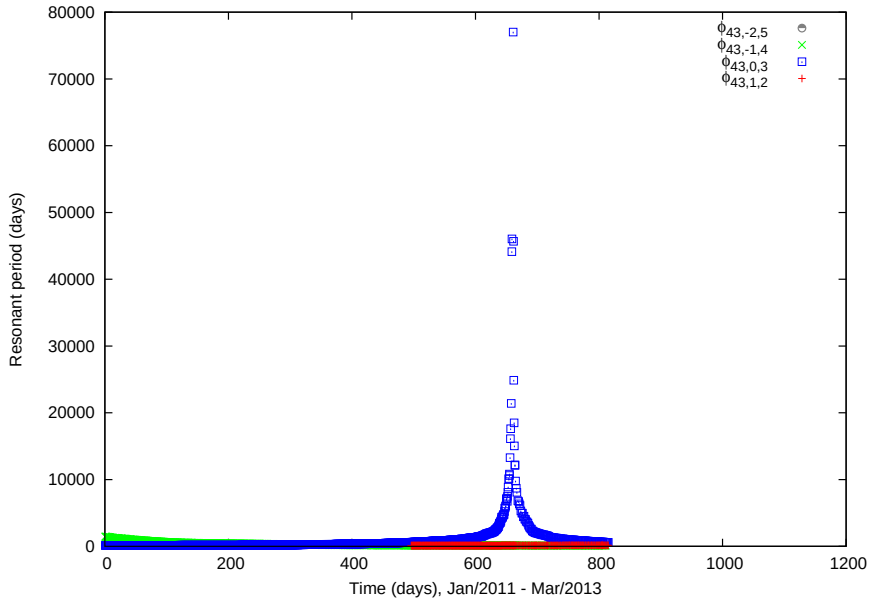

Figure 5: Time behavior of the resonant period: Orbital motion of the artificial satellite CBERS-1 corresponding to January/2011 to March/2013.

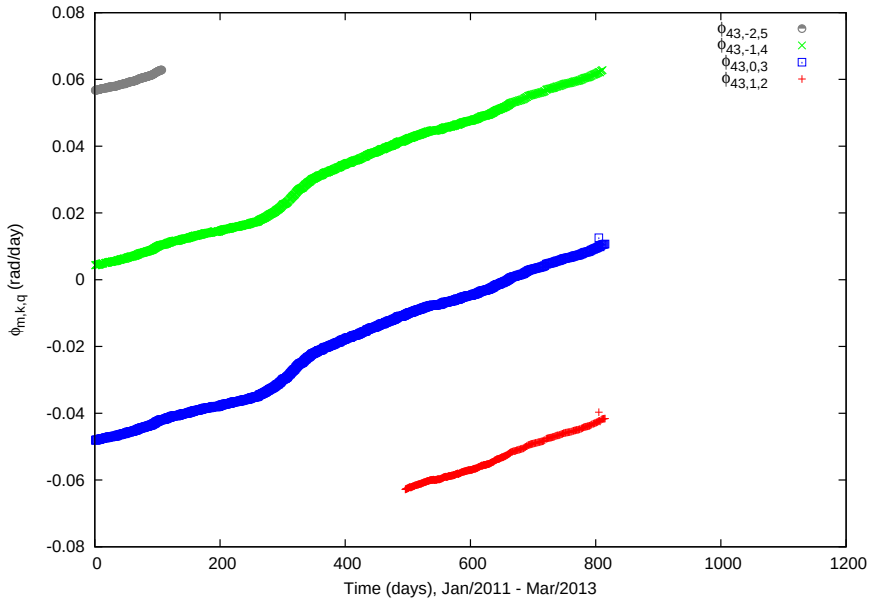

Figure 6: Time behavior of the $\dot{\phi}_{kmq}$: Orbital motion of the artificial satellite CBERS-1 corresponding to January/2011 to March/2013.

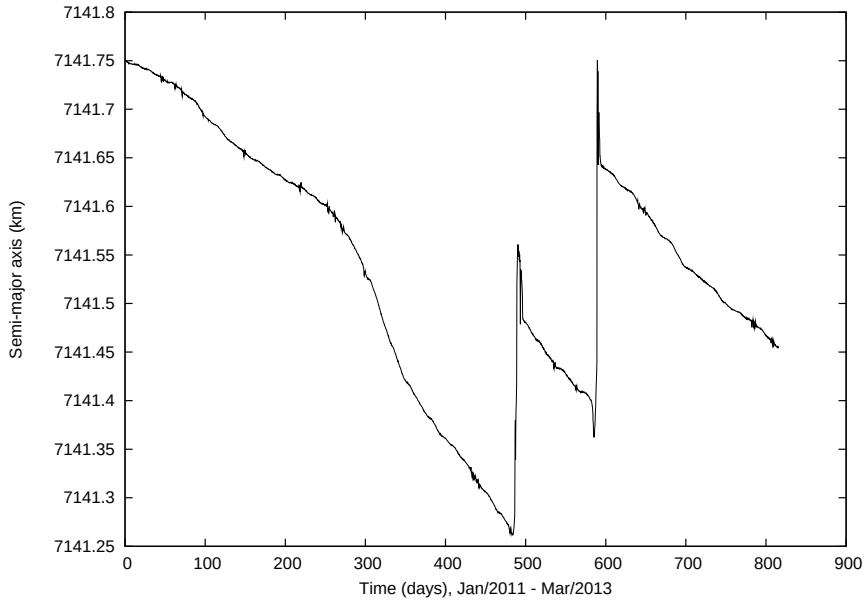

Figure 7: Time behavior of the semi-major axis: Orbital motion of the artificial satellite CBERS-2 corresponding to January/2011 to March/2013.

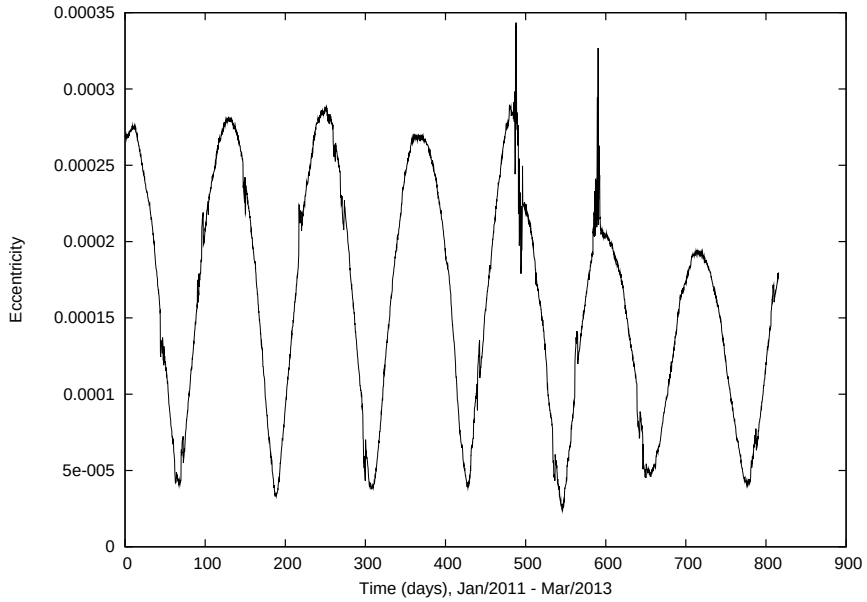

Figure 8: Time behavior of the eccentricity: Orbital motion of the artificial satellite CBERS-2 corresponding to January/2011 to March/2013.

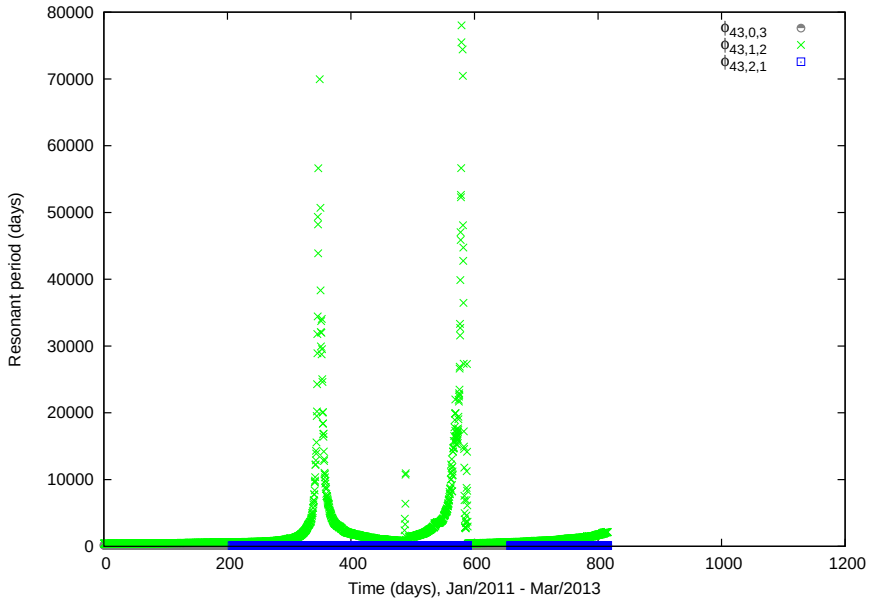

Figure 9: Time behavior of the resonant period: Orbital motion of the artificial satellite CBERS-2 corresponding to January/2011 to March/2013.

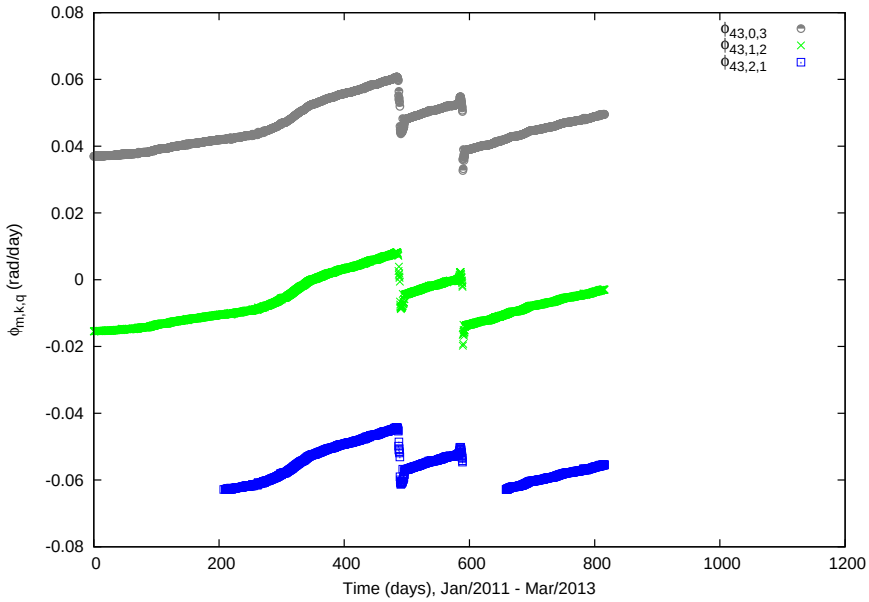

Figure 10: Time behavior of the $\dot{\phi}_{kmq}$: Orbital motion of the artificial satellite CBERS-2 corresponding to January/2011 to March/2013.

4. Kozai's resonance

In this section, the orbital motions of CBERS-1 and CBERS-2 satellites are studied in the (ω, e) plane, observing the presence of Kozai's resonance. Where ω is the argument of pericentre and e is the eccentricity. This kind of phenomenon was first observed by Kozai (1962), [24], and Lidov (1962), [25], and it is known as the Lidov- Kozai's mechanism. The Lidov-Kozai's mechanism has been studied for Jupiter's satellites as in Yokoyama et. al. (2003), [26], for asteroids as in Kozai (1962), [24], for Uranus's satellites as Kinoshita and Nakai (1999, 2007), [27, 28] and for artificial satellite orbiting the Earth as in Sampaio and Vilhena de Moraes (2012) [29].

To verify the Lidov-Kozai's mechanism in a specified orbital motion, curves of same energy in the (ω, e) plane is verified showing libration and circulation curves. The study of the Lidov-Kozai's mechanism is based on the parameter h, related with the z component of the angular momentum. The parameter h is given by:

$$h = (1 - e^2)cos^2(I) = const. \tag{11}$$

where I is the inclination of the orbit plane with the equator.

Figures 11 to 14 show the (ω, e) plane using the TLE data of the CBERS-1 and CBERS-2 satellites. Figure 11 shows circulation region in the (ω, e) plane for CBERS-1 in the period January/2011 to March/2013. Figure 12 shows circulation and libration regions considering the orbital motion of CBERS-1 in the period October/1999 to March/2013, analyzing real data since launch. Figure 13 shows circulation and libration regions in the (ω, e) plane for CBERS-2 in the period January/2011 to March/2013. Figure 14 shows circulation and libration regions considering the orbital motion of CBERS-2 in the period October/2003 to March/2013, analyzing real data since launch.

This analysis is very important and interesting because it shows a new perspective to study objects in LEO region. This analysis helps to find stable regions in the orbital motions around the Planet.

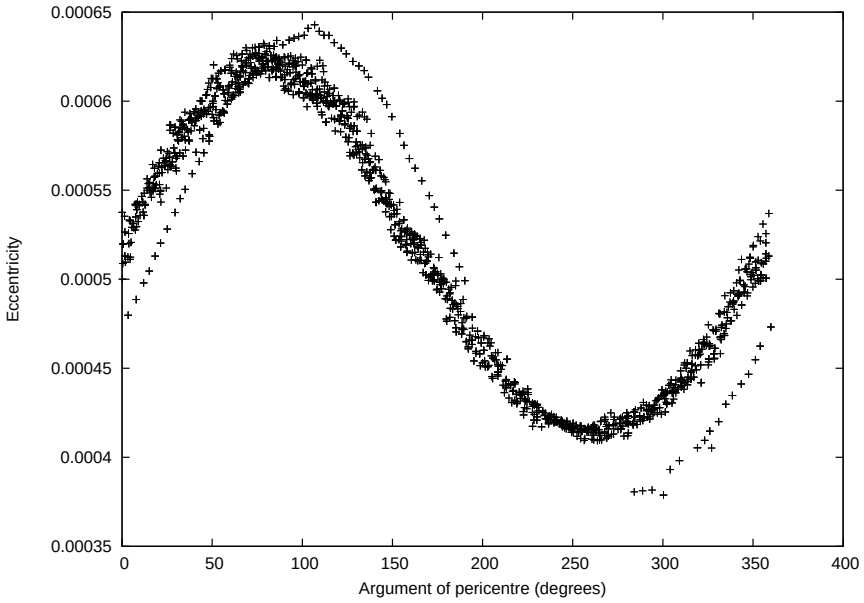

Figure 11: Argument of pericentre versus eccentricity: Orbital motion of the artificial satellite CBERS-1 corresponding to January/2011 to March/2013.

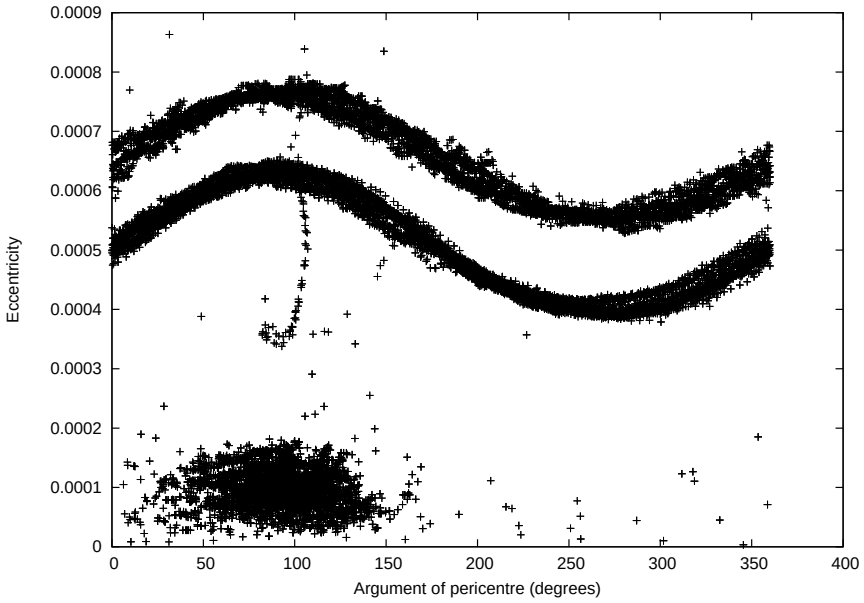

Figure 12: Argument of pericentre versus eccentricity: Orbital motion of the artificial satellite CBERS-1 corresponding to October/1999 to March/2013.

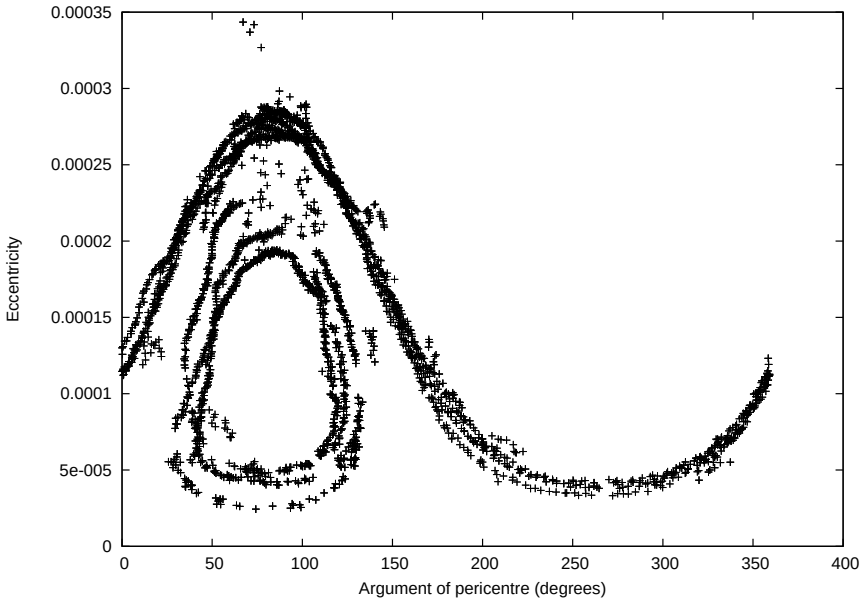

Figure 13: Argument of pericentre versus eccentricity: Orbital motion of the artificial satellite CBERS-2 corresponding to January/2011 to March/2013.

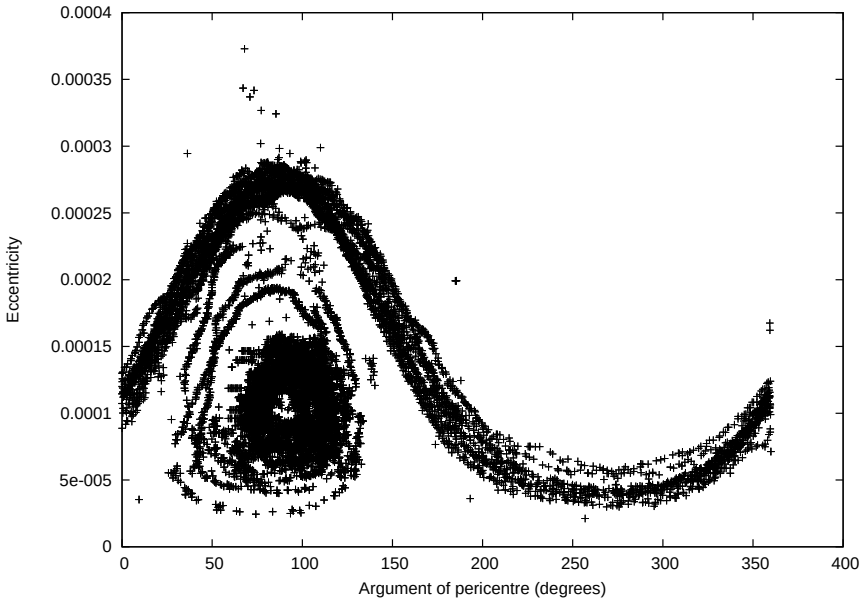

Figure 14: Argument of pericentre versus eccentricity: Orbital motion of the artificial satellite CBERS-2 corresponding to October/2003 to March/2013.

5. Conclusions

In this work, resonant orbital motions of the CBERS (China-Brazil Earth Resource Satellite) satellites are studied using the TLE files of the NORAD.

The orbital motions of the CBERS satellites can be corrected during your lifetime, because some disturbances, resonance effects or collision risk can affect your mission. These corrections can be seen by the abrupt change in the values of the semi-major axis. In this way, the study of the resonant angles using real data of the artificial satellites is limited to the period without corrections. However, the study involving space debris allows to use a long time and consequently a better analysis about the resonant period in a given region.

The results and discussions show the complexity, in the orbital dynamics of these objects, caused by the resonance effects. Figures show time behavior of the semimajor axis, eccentricity, resonant angles and resonant periods.

Energy's curves are observed in the $(\omega; e)$ plane of the orbital motions of CBERS-1 and CBERS-2 satellites indicating the presence of Kozai's resonance in their orbits. Where ω is the argument of pericentre and e is the eccentricity.

The TLE catalog of objects orbiting the Earth is an important tool to study the orbital motion of the artificial satellites and space debris.

ACKNOWLEDGEMENTS

This work was accomplished with support of the FAPESP under the contracts N^o 2012/24369-0 and 2012/21023-6, SP-Brazil, and CNPQ (contract 303070/2011-0) and CAPES.

References

[1] R. Osiander, P. Ostdiek, Introduction to Space Debris, Handbook of Space Engineering, Archeology and Heritage, 2009.

[2] H. Ikeda, T. Hanada, T. Yasaka, Searching for lost fragments in GEO, Acta Astronautica 63 (2008) 1312–1317.

[3] Space Track. Archives of the 2-lines elements of NORAD. Available at: <www.space-track.org>, accessed in August - November, 2013.

[4] H. K. Kuga, Use of the ephemeris "2-lines" from NORAD in the orbital motion of the CBERS-1 satellite, I Congress of Dynamics, Control and Applications, Issue 1 (2002) 925-930 (in Portuguese).

[5] V. Orlando, R. V. F. Lopes, H. K. Kuga, Flight dynamics team experience throughout four years of SCD1 in-orbit operations: main issues, improvements and trends, in: Proceedings of XII International Symposium on Space Flight Dynamics, Darmstadt, Germany, ESOC, 1997, pp. 433-437.

[6] F. R. Hoots, R. L. Roehrich, Models for Propagation of NORAD Element Sets, Spacetrack Report N^o. 3, 1980.

[7] Z. Changyin, Z. Wenxiang, H. Zengyao, W. Hongbo, Progress in space debris research, Chinese Journal of Space Science 30 (2010) 516-518.

[8] S. Nishida, S. Kawamoto, Y. Okawa, F. Terui, S. Kitamura, Space debris removal system using a small satellite, Acta Astronautica 65 (2009) 95-102.

[9] M. J. Mechishnek, Overview of the Space Debris Environment, AEROSPACE REPORT NO. TR-95(5231)-3, 1995.

[10] M. T. Lane, An Analytical Treatment of Resonance Effects on Satellite Orbits, Celestial Mechanics 42 (1988) 3-38.

[11] D. M. Sanckez, T. Yokoyama, P. I. O. Brasil, R. R. Cordeiro, Some Initial Conditions for Disposed Satellites of the Systems GPS and Galileo Constellations, Mathematical Problems in Engineering, 2009.

[12] L. D. D. Ferreira and R. Vilhena de Moraes, "GPS Satellites Orbits: Resonance", Mathematical Problems in Engineering, Vol. 2009.

[13] A. Rossi, Resonant dynamics of Medium Earth Orbits: space debris issues, Celestial Mechanics and Dynamical Astronomy 100 (2008) 267–286.

[14] F. Deleflie, A. Rossi, C. Portman, G. Métris, F. Barlier, Semi-analytical investigations of the long term evolution of the eccentricity of Galileo and GPS-like orbits, Advances in Space Research 47, Issue 5 (2011) 811-821.

[15] L. Anselmo, C. Pardini, Dynamical evolution of high area-to-mass ratio debris released into GPS orbits, Advances in Space Research 43, Issue 10 (2009) 1491-1508.

[16] C. C. Chao, R. A. Gick, Long-term evolution of navigation satellite orbits: GPS/GLONASS/GALILEO, Advances in Space Research 34, Issue 5 (2004) 1221-1226.

[17] J. C. Sampaio, R. Vilhena de Moraes, S. S. Fernandes, Artificial Satellites Dynamics: Resonant Effects, in: Proceedings of the 22nd International Symposium on Space Flight Dynamics, São José dos Campos, 2011.

[18] J. C. Sampaio, R. Vilhena de Moraes, S. S. Fernandes, The Orbital Dynamics of Synchronous Satellites: Irregular Motions in the 2:1 Resonance, Mathematical Problems in Engineering, 2012a.

[19] J. C. Sampaio; A. G. S. Neto; S. S. Fernandes; R. Vilhena de Moraes; M. O. Terra, Artificial satellites orbits in 2:1 resonance: GPS constellation. Acta Astronautica 81, (2012b) 623–634.

[20] J. C. Sampaio, E. Wnuk, R. Vilhena de Moraes, S. S. Fernandes, Resonant Orbital Dynamics in LEO Region: Space Debris in Focus, Mathematical Problems in Engineering, 2014.

[21] L. Anselmo, C. Pardini, Orbital evolution of the first upper stages used for the new European and Chinese navigation systems, Acta Astronautica 68 (2011) 2066 - 2079.

[22] CBERS Satellites. Archives of the CBERS Satellites. Available at: <www.cbers.inpe.br>, accessed in August, 2013.

[23] J. Golebiwska, E. Wnuk, I. Wytrzyszczak, Space debris observation and evolution predictions, Software Algorithms Document (SAD), ESA PECS Project N^o 98088, Astronomical Observatory of the Adam Mickiewicz University, Poznan, 2010.

[24] Kozai, Y. Secular Perturbations of Asteroids with High Inclination and Eccentricity. Massachusetts, The Astronomical Journal, vol. 67, n0 9, 1962.

[25] Lidov, M. L. The evolution of orbits of artificial satellites of planets under the action of gravitational perturbation of external bodies. Planet. Space Sci. 9, 1962, 719-759 (The English translation of Lidov's paper (1961))

[26] Yokoyama, T.; Santos. M. T.; Cardin, G.; Winter, O. C. On the orbits of the outer satellites of Jupiter. Astronomy and Astrophysics 401, 2003, 763-772.

[27] Kinoshita, H.; Nakai, H. Analytical Solution of the Kozai Resonance and its Application Celestial Mech Dyn Astr 75, 1999, 125-147.

[28] H. Kinoshita; H. Nakai. General solution of the mechanism Celestial Mech Dyn Astr 98, 2007, 67-74.

[29] J. C. Sampaio; R. Vilhena de Moraes. ARTIFICIAL SATELLITES: RESONANCE EFFECTS PRODUCED BY TERRESTRIAL TIDE. Journal of Aerospace Engineering, Sciences and Applications, Jan. – Mar. 2012, Vol. IV, No 1.